



The birth of aposematism: High phenotypic divergence and low genetic diversity in a young clade of poison frogs



Rebecca D. Tarvin^{a,1,*}, Emily A. Powell^{a,b,1}, Juan C. Santos^{c,d}, Santiago R. Ron^e, David C. Cannatella^a

^a Department of Integrative Biology and Biodiversity Collections, University of Texas, Austin, TX, United States

^b Department of Biology, University of Miami, Miami, FL, United States

^c Department of Biology, Brigham Young University, Provo, UT, United States

^d Department of Biological Sciences, St. John's University, Queens, NY, United States

^e Museo de Zoología, Escuela de Biología, Pontificia Universidad Católica del Ecuador, Quito, Ecuador

ARTICLE INFO

Article history:

Received 4 August 2016

Revised 30 November 2016

Accepted 28 December 2016

Available online 13 January 2017

Keywords:

Species delimitation

Phenotypic divergence

Introgression

Warning signals

Polymorphism

Multispecies coalescent method

ABSTRACT

Rapid radiation coupled with low genetic divergence often hinders species delimitation and phylogeny estimation even if putative species are phenotypically distinct. Some aposematic species, such as poison frogs (Dendrobatidae), have high levels of intraspecific color polymorphism, which can lead to overestimation of species when phenotypic divergence primarily guides species delimitation. We explored this possibility in the youngest origin of aposematism (3–7 MYA) in poison frogs, *Epipedobates*, by comparing genetic divergence with color and acoustic divergence. We found low genetic divergence (2.6% in the 16S gene) despite substantial differences in color and acoustic signals. While chemical defense is inferred to have evolved in the ancestor of *Epipedobates*, aposematic coloration evolved at least twice or was lost once in *Epipedobates*, suggesting that it is evolutionarily labile. We inferred at least one event of introgression between two cryptically colored species with adjacent ranges (*E. boulengeri* and *E. machalilla*). We also find evidence for peripheral isolation resulting in phenotypic divergence and potential speciation of the aposematic *E. tricolor* from the non-aposematic *E. machalilla*. However, we were unable to estimate a well-supported species tree or delimit species using multispecies coalescent models. We attribute this failure to factors associated with recent speciation including mitochondrial introgression, incomplete lineage sorting, and too few informative molecular characters. We suggest that species delimitation within young aposematic lineages such as *Epipedobates* will require genome-level molecular studies. We caution against relying solely on DNA barcoding for species delimitation or identification and highlight the value of phenotypic divergence and natural history in delimiting species.

© 2017 Elsevier Inc. All rights reserved.

1. Introduction

In the face of the rapid loss of biodiversity, efforts to attain a more complete catalog and phylogeny of living organisms have intensified, especially in diverse tropical regions (Myers et al., 2000; Vieites et al., 2009). Among those groups, amphibians are a priority as they have experienced a rapid decline, with over a third of species recognized as globally threatened (Stuart et al., 2004). Although there is a general consensus that a species constitutes a

separately evolving set of populations (metapopulation) under the General Lineage Concept (de Queiroz, 2007), there are many competing criteria and methods for delimiting species. However, the application of these procedures on recently diverged species remains particularly difficult because incomplete lineage sorting (ILS) and introgression, often associated with low genetic divergence, can obfuscate reconstructing well supported trees (Fouquet et al., 2007; Hebert et al., 2004; Reid and Carstens, 2012; Vieites et al., 2009). Multispecies coalescent methods (MSCs) bolster inferences in cases of low genetic divergence by taking into account the timing of allele coalescence across loci (Fujita et al., 2012; Yang, 2015a). However, MSCs are currently limited to molecular data (de Queiroz, 2007, 2005), but the best species-delimitation methods should be integrative, adding evidence from morphology, behavior, and ecology (Dayrat, 2005).

Although species delimitation is challenging in the case of phenotypically similar (“cryptic”) species, it may also be difficult if the

Abbreviations: bpp, Bayesian Posterior Probabilities; BP&P, Bayesian Phylogenetics and Phylogeography program; ML, Maximum Likelihood; ILS, Incomplete Lineage Sorting; TNHCFS, Texas Natural History Collections Field Series; MSC, MultiSpecies Coalescent; SNP, Single Nucleotide Polymorphism; MYA, million years ago; HPD, Highest Posterior Density.

* Corresponding author.

E-mail address: rdtarvin@gmail.com (R.D. Tarvin).

¹ Authors contributed equally.

metapopulations of a putative species have recently diverged phenotypically. For example, aposematic species that use visual signals to warn predators of their defenses often co-opt these signals for intraspecific communication, leading to high intraspecific color variation (Cumplings and Crothers, 2013; Merrill et al., 2014). Consequently, taxonomists may divide one polymorphic species into multiple species (over-splitting) or describe a new species based on a newly observed color morph (e.g., Cisneros-Heredia and Yáñez-Muñoz, 2010; Perez-Peña et al., 2010; Posso-Terranova and Andrés, 2016). Such delimitations may or may not reflect reproductive isolation and might introduce human perception bias in classification of visually distinct populations (e.g., color morphs) even if different morphs can sometimes interbreed (Brusa et al., 2013; Hauswaldt et al., 2011; Medina et al., 2013; Summers et al., 2004; Yang et al., 2016). Thus, the taxonomic status of putative species with small ranges, low genetic divergence, and no evidence of reproductive isolation should be questioned. Here we explore this problem by addressing molecular and phenotypic divergence in the youngest (3–7MYA) clade of aposematic poison frogs, *Epipedobates* (Santos et al., 2009).

Epipedobates is a small clade of seven nominal species that occupy lowlands west of the Andes from southern Colombia to northern Peru (Fig. 1). Chemical defense occurs via dietary uptake of alkaloids, along with other phenotypic adaptations including high aerobic capacity and conspicuous coloration (Santos and Cannatella, 2011). Four of the seven *Epipedobates* species exhibit bright coloration associated with defense; only one species (*E. machalilla*) is considered to be undefended and inconspicuous (Santos et al., 2009; Santos and Cannatella, 2011). This genus presents a challenging case for species delimitation because despite divergent mating calls and phenotypic differences that readily identify the species (Graham et al., 2004; Santos et al., 2014), all previous studies have recovered inconsistent phylogenies with low node support, failing to resolve species-level relationships (Clough and Summers, 2000; Grant et al., 2006; Santos, 2012; Santos et al., 2014, 2009, 2003; Vences et al., 2003); however, none of these sampled more than three populations or a handful of specimens.

Increasing the number of loci, populations, and individuals will generally improve phylogenetic inference and species delimitation (Knowles and Carstens, 2007). However, Santos and Cannatella (2011) used ~10,000 nt (eight mitochondrial and seven nuclear genes), and found very short branches separating the single individuals of five *Epipedobates* species. Moreover, studies including more populations per species but fewer loci recovered non-monophyly of *E. boulengeri* and *E. machalilla* (Grant et al., 2006; Santos et al., 2009). Thus, our aims were to address the species limits and phylogenetic relationships within *Epipedobates* by using more individuals and populations to characterize phenotypic divergence and estimate species trees. We sequenced 3 genes for at least 15 individuals per species (72 individuals total) from 9 populations of 4 species of *Epipedobates*. We estimated a new phylogeny and quantified divergence in coloration among all individuals. We also evaluated existing acoustic data in light of documented color and genetic divergence. We discuss phylogenetic and phenotypic patterns occurring in the early origins of aposematism and the implications for species delimitation in polymorphic aposematic lineages.

2. Material and methods

2.1. Specimen collection

Seven species of *Epipedobates* are recognized. Individuals of four species of *Epipedobates* (*E. boulengeri* from 2 populations,

17 individuals; *E. tricolor* from 2 populations, 16 individuals; *E. machalilla* from 2 populations, 16 individuals; *E. anthonyi* from 3 populations, 23 individuals) were collected by RDT and SRR under the permit N° 001-11 IC-FAU-DNB/MA from the Ecuadorian Ministry of the Environment at various sites across Western Ecuador in July 2012 (see Supplementary Table S1 for voucher information; Fig. 1). However, we did not collect individuals of *E. darwinwallacei*, *E. espinosai*, and *E. narinensis*, all of which have restricted ranges. We followed protocols approved by the University of Texas at Austin (IACUC No. AUP-2012-00032). Liver tissue samples were removed from euthanized animals and stored in 95% ethanol. All voucher specimens are deposited in the Museo de Zoología de Pontificia Universidad Católica del Ecuador (QCAZ at PUCE). Genetic material from 11 other species was obtained from the Genetic Diversity Collection (part of the Biodiversity Collections) of University of Texas at Austin.

2.2. DNA sequencing and alignment

DNA was extracted from liver tissues using Qiagen DNeasy Blood & Tissue kits (Valencia, CA). Two mitochondrial genes were amplified using published protocols and primer sequences (Goebel et al., 1999; Santos et al., 2003; Santos and Cannatella, 2011); the primer names follow Santos et al. (2003). The first gene, a segment overlapping the end of 12S and the beginning of 16S, was amplified with primers 12L1-L (5'-AAAAAGCTTCAAAGTGGAT TAGATACCCACTAT-3') and 16SH-H (5'-GCTAGACCATGATG CAAAAGGTA-3') using a 2-min initial denaturation at 94 °C, followed by 40 cycles of 30 s at 94 °C, 30 s at 48 °C, 1 min at 72 °C, and a final extension time of 7 min at 72 °C. The second, *Cytochrome B*, was sequenced with primers Den3-L (5'-AAYATYTC CRYATGATGRAAYTYGG) and Den1-H, (5'-GCRAANAGRAAGTAT CATTNCGGYTTRAT) using the same protocol. Annealing temperatures were lowered to 46.5 °C for individuals that were difficult to amplify. The nuclear gene encoding voltage-gated potassium channel 1.3 (*Kv1.3*) was sequenced with primers Kv13_8F (5'-GG TGGCGTGTGATAACATCC) and Kv13_1497R (5'-ACATCGGTAAA GATCTTCTTGATA) (designed by RDT), using a 2-min initial denaturation at 94 °C, followed by 40 cycles of 30 s at 94 °C, 30 s at 52 °C, 1 min 30 s at 72 °C, and a final extension time of 7 min at 72 °C. A different downstream region of 16S is more often used for phylogenetic analysis and barcoding (Vences et al., 2004). To compare our data with those of other studies, we also sequenced this region of 16S in 10 individuals using the primers 16SC (5'-GTRGGCCTAAAA GCAGCCAC-3) and 16SD (5'-CTCCGGTCTGAACTCAGATCACGTAG-3) (Santos et al., 2003) and the mtDNA protocol described above. All samples were sequenced with forward and reverse primers at the Institute for Cellular and Molecular Biology Core Facility at the University of Texas at Austin. The outgroup taxa were sequenced for the same markers using the same described laboratory protocol or they were obtained from GenBank (see accession numbers in Supplementary Table S1). Sequence quality was assessed in Sequencher v4.7 (Ann Arbor, MI); we report consensus sequences of forward and reverse reads. These were first aligned using MUSCLE (Edgar, 2004) and then adjusted in Mesquite (Maddison and Maddison, 2015). Alignments are provided as Supplementary Datasets 1–4. *Cytochrome B* and *Kv1.3* alignments were translated to amino acids and adjusted to assure that codons were in-frame. Low-quality sequence ends and gaps were excluded (90 nt) from the total 2803-nt alignment. Our selection of excluded sites only differed by 18 nt from that predicted by Gblocks v0.91b (Castresana, 2000), so we use our original selection of excluded sites in all analyses. Variable sites and parsimony-informative sites were identified with MEGA v4 (Kumar et al., 2008).

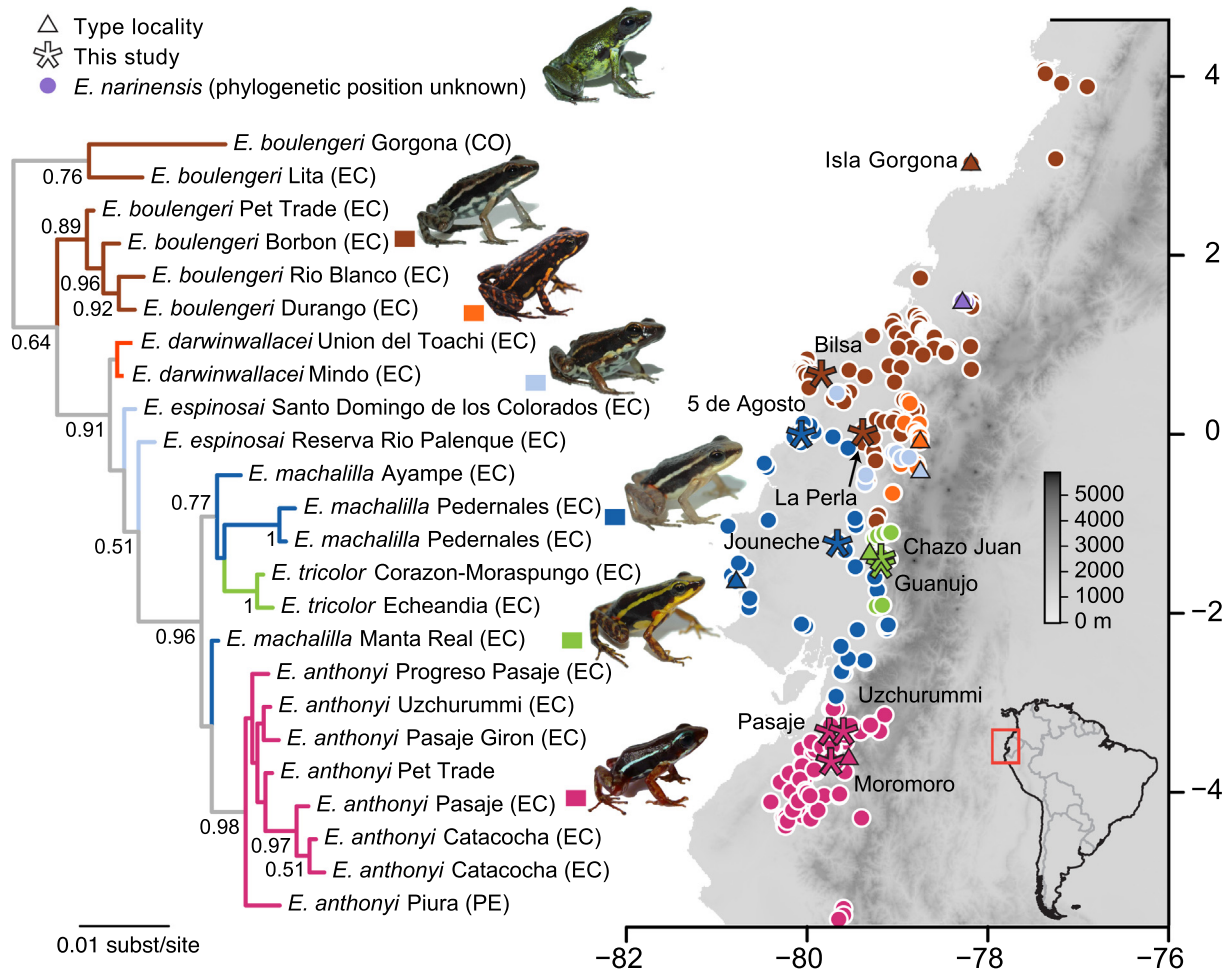


Fig. 1. The seven species of *Epipedobates* range from northern Peru to southern Colombia. The stars indicate nine populations from which 72 individuals of 4 species were sampled. The filled circles mark collection sites from museum records (see [Supplementary Table S10](#)) and triangles indicate type localities. The MrBayes phylogeny was constructed from *Epipedobates* mtDNA sequences currently available in GenBank; bpp support values >0.50 are shown. EC, Ecuador; PE, Peru; CO, Colombia. Voucher specimen numbers for photographs: *E. anthonyi*, QCAZA53675; *E. boulengeri*, QCAZA58239; *E. darwinwallacei*, QCAZA58284; *E. espinosai*, QCAZA58270; *E. machalilla*, QCAZA58291; *E. narinensis*, RDT0222; and *E. tricolor*, QCAZA58307.

2.3. Phylogeny estimation

We estimated a phylogeny using the concatenated alignment (2803 nt total) with maximum likelihood in RAxML v8 (Stamatakis, 2014) and Bayesian inference in MrBayes 3.2.6 (Ronquist et al., 2012; Ronquist and Huelsenbeck, 2003). The best partition scheme was determined using the autopartition command in PAUP* v4.0a149 (Swofford, 2002), which supported separate partitions for each gene as well as for each codon position in protein-coding genes *Cytochrome B* and *Kv1.3*. Appropriate models for RAxML were selected using jModelTest v2.0 (Durriba et al., 2012); both GTR + G + I and GTR + G scored highly. Although the substitution model GTR + G + I was selected by jModelTest, GTR + G was used as recommended by Stamatakis (2014). The Bayesian analysis was conducted with four chains and two runs of ten million generations each with a temperature of 0.08, a burn-in of 25%, and a sampling frequency of 500. The temperature parameter was set to 0.08, which ensured that acceptance ratios for hot-cold chain swapping were <80% and >30%. We used nst = mixed, which samples over the space of all possible reversible substitution models of the rate matrix parameters (Ronquist et al., 2012), and estimated the alpha parameter of the gamma distribution (rates = gamma) and the base frequencies. The branch-length prior was set to optimize the sampling of short branch lengths

(brlenspr = unconstrained:exponential(200); Marshall, 2010). We report node support from 1000 bootstraps in RAxML and as Bayesian Posterior Probabilities (bpp) from the MrBayes runs. Node support values were defined as weak (0.50–0.74 for Bayesian posterior probabilities and 50–74% bootstrap proportions), moderate (0.75–0.94 bpp, 75–94% bootstrap) or strong (0.95–1.00 bpp, 95–100% bootstrap). Values <50 for node support were considered very weak.

To place our four target species in context with the entire *Epipedobates* clade, we downloaded all 12S–16S sequences of *Epipedobates* available in Genbank (27 individuals representing six of seven *Epipedobates* species – no sequences have been published for *E. narinensis*; [Supplementary Table S1](#)). We trimmed the alignment to contain only the 770-base subset of the 12S–16S gene region, corresponding roughly to site 450 of the 12S gene extending through the *tRNA-val* gene and the first 160 bp of the 16S gene. Twenty-seven sites of mostly single-base insertions were excluded. We used *Ameerega bilinguis*, *Silverstoneia aff. nubicola*, and *Colostethus fugax* as outgroups to root the *Epipedobates* tree. We estimated a phylogeny in MrBayes v3.2.6 using the priors described above, treating the fragment as one partition. Stationarity was reached in 1,000,000 generations. All ESS values were >500, and the average standard deviation of split frequencies was 0.0069. The 95% credible set (highest posterior density) contained 2850

trees, consistent with poor support for several nodes. We report node support as Bayesian posterior probabilities (bpp) from MrBayes.

2.4. Pairwise genetic distances and haplotype network analyses

Pairwise distances between individuals were computed separately for each gene and for the concatenated matrix using uncorrected p-values in MEGA v7 (Kumar et al., 2008). Haplotypes of the nuclear gene *Kv1.3* were reconstructed using PHASE v2.1 software (Stephens et al., 2001; Stephens and Donnelly, 2003) implemented in DnaSP v5.10.1 (Librado and Rozas, 2009). We then estimated haplotype networks for the concatenated mitochondrial genes (*Cytochrome B* and *12S–16S*) and for the nuclear gene (*Kv1.3*) using the Median Joining Network algorithm (Bandelt et al., 1999) in PopART (<http://popart.otago.ac.nz>). For the network analysis, we split the Bilsa population of *E. boulengeri* into two haplotype groups (Bilsa A and Bilsa B; see Fig. 2) because phylogenetic analysis of mtDNA recovered a deep divergence between these individuals, which are from the same population (Bilsa).

2.5. Species-tree estimation

We estimated species trees using the Bayesian MSC method in BP&P v3.2 (Rannala and Yang, 2003; Yang, 2015a), which estimates gene-tree topologies and branch lengths and incorporates uncertainty in allele coalescence to identify the species tree with the highest posterior probability. We used two models to predict species trees: the A01 model, which holds “species” delimitations (or populations in our case) constant (speciesdelimitation = 0) and estimates the species tree (speciestree = 1), and the A11 model, which co-estimates assignment of individuals to a population/species (speciesdelimitation = 1) and the species tree (speciestree = 1). In all analyses we allowed for variation in mutation rate across loci (locusrate = 1, with Dirichlet distribution parameter $\alpha = 2.0$) and specified a heredity multiplier for each nuclear (=1.0) and mitochondrial (=0.5) locus (heredity = 2). We used an informative prior of $\tau \sim G(32.6, 1000)$ for divergence time (uncorrected p-distance at root of clade = 0.0326) and a more diffuse prior for population size $\theta \sim G(2, 100)$, both measured in expected number of mutations per site (where $\theta = 4N\mu \approx$ average pairwise difference = 0.02; Yang, 2015b).

Following suggestions of the BP&P authors, we used priors that yielded acceptance proportions >0.15 and <0.70 for MCMC moves (see Yang, 2015b, p. 12), employed both reverse-jump MCMC (rjMCMC) methods 0 and 1 (see below), and ran multiple analyses with different starting trees to ensure that the program converged on the most probable result (Yang, 2015a; Yang and Rannala, 2010). Thus, we first ran preliminary analyses with 10,000 generations using rjMCMC (burn-in = 4000, sampling frequency = 2, speciesdelimitation = 1, method = 0 with fine-tune parameter $\varepsilon = 2.5$; see Yang and Rannala (2010)) to determine appropriate priors for the parameters finetune and speciesmodelprior; successful convergence of chains required that the τ finetune parameter be set to 0.001 and that the speciesmodelprior be set to 1 (indicating equal probability for all possible rooted species trees). These preliminary analyses were also run excluding individuals with missing data; however, the same results were obtained in either case, so all individuals were used subsequently. We then ran additional preliminary analyses with three different starting trees (the Bayesian tree topology, a second similar tree with Bilsa population individuals constrained to be monophyletic, and a third tree constrained to exclude bipartitions present in the Bayesian tree); the choice of starting tree did not affect results, so we used the Bayesian tree topology as a prior. Preliminary ML and Bayesian analyses revealed a deep split among individuals of the *E. boulengeri* Bilsa population.

Therefore, we ran final analyses with all Bilsa individuals assigned to one population (number of “species” = 9) and with Bilsa individuals split into genetic populations A and B (number of “species” = 10). Final analyses were run four times with 50,000 generations (burn-in = 5000, sampling frequency = 4) using both rjMCMC methods 0 (with finetune parameter $\varepsilon = 20$) and 1 (with finetune parameters $\alpha = 1$ and $m = 2$).

We used TreeAnnotator from the BEAST software package (Drummond et al., 2012) to summarize A01 results from BP&P. For each analysis (i.e., 9 populations or 10 populations), we combined results from all four runs and estimated the Maximum Clade Credibility tree and 95% High Density Posterior estimates of τ (tau, divergence time) using 0% burn-in (BP&P discards burn-in before recording results). Scale was converted from number of expected substitutions per site to MY with an estimated mutation rate of Amphibia as $\mu \approx 0.00345$ subs/site/MY (Santos et al., 2009) using the following calculation: τ (~MY) = τ (subs/site)/ μ (subs/site/MY) (Yang, 2015a). We also converted population size (θ) estimates from expected number of substitutions per site to effective population size (N_e) using the following equation: θ (N_e) = θ (subs/site)/ 4μ (subs/site/MY) $\times 1,000,000$ Y (Yang, 2015a).

2.6. Phenotypic analysis

Detailed methods and additional analyses can be found in Tarvin et al. (in review). Briefly, three digital color photographs (dorsal, ventral, and lateral views) were taken of each individual without flash using a Panasonic DMC-FH20 digital camera and an 18% Gray card (Kodak Gray Card/R-27 19003061) to allow standardization of light levels. Each photograph was partitioned in Photoshop® into 6–8 regions based on color pattern. Each region was then split into red, green, and blue channels in ImageJ v1.48 (Schneider et al., 2012); percent area and average red, green, and blue intensity of each region of the frog were measured. From these, two color channels and one luminance channel were computed following Endler (2012). These calculations yielded 76 variables representing color and pattern diversity across 72 *Epipedobates* individuals. We excluded individual TNHCF56818 in these analyses because photographs were taken >20 min post-mortem. We calculated pairwise Euclidean distances among individuals in R v3.0.2 with dist() from the package stats, and graphed these against pairwise genetic distances (using all 2803 nt) as dendrograms using hierarchical clustering in hclust() in the stats package (with method = “average”) and tanglegram() in the dendextend package (Galili, 2015; R Core Team, 2016).

2.7. Acoustic analysis

We obtained mating call data of *Epipedobates* and two closely related genera (*Colostethus* and *Silverstoneia*) from Santos et al. (2014, their Supplementary Table S1). Calls used in our analyses are deposited at the Cornell Lab of Ornithology’s Macaulay Library (Accession ACC3643; see Supplementary Table S2). We excluded variables describing multi-note parameters because these cannot be homologized unequivocally to single-note calls. Instead, we created a binary variable describing whether each call was single-note or multi-note. To reduce the number of variables, we identified and removed variables with correlation coefficients >99% using the cor() function in the R v3.0.2 stats package (R Core Team, 2016). Our final set of 12 acoustic variables included the Unit-of-Repetition Interval (s, seconds), the Number of Initial Pulse Notes, the Initial-Pulse Duration (s), the Initial-Pulse Interval (s), the Initial-Peak Frequency (Hz, hertz), the Number of Middle-Pulse Notes, the Middle-Pulse Duration (s), the Middle-Pulse Interval (s), the Middle-Pulse Rise Time (s), the Middle-Pulse Shape, the Middle-Pulse Duty, and the Middle-Peak Frequency (Hz) (see Santos

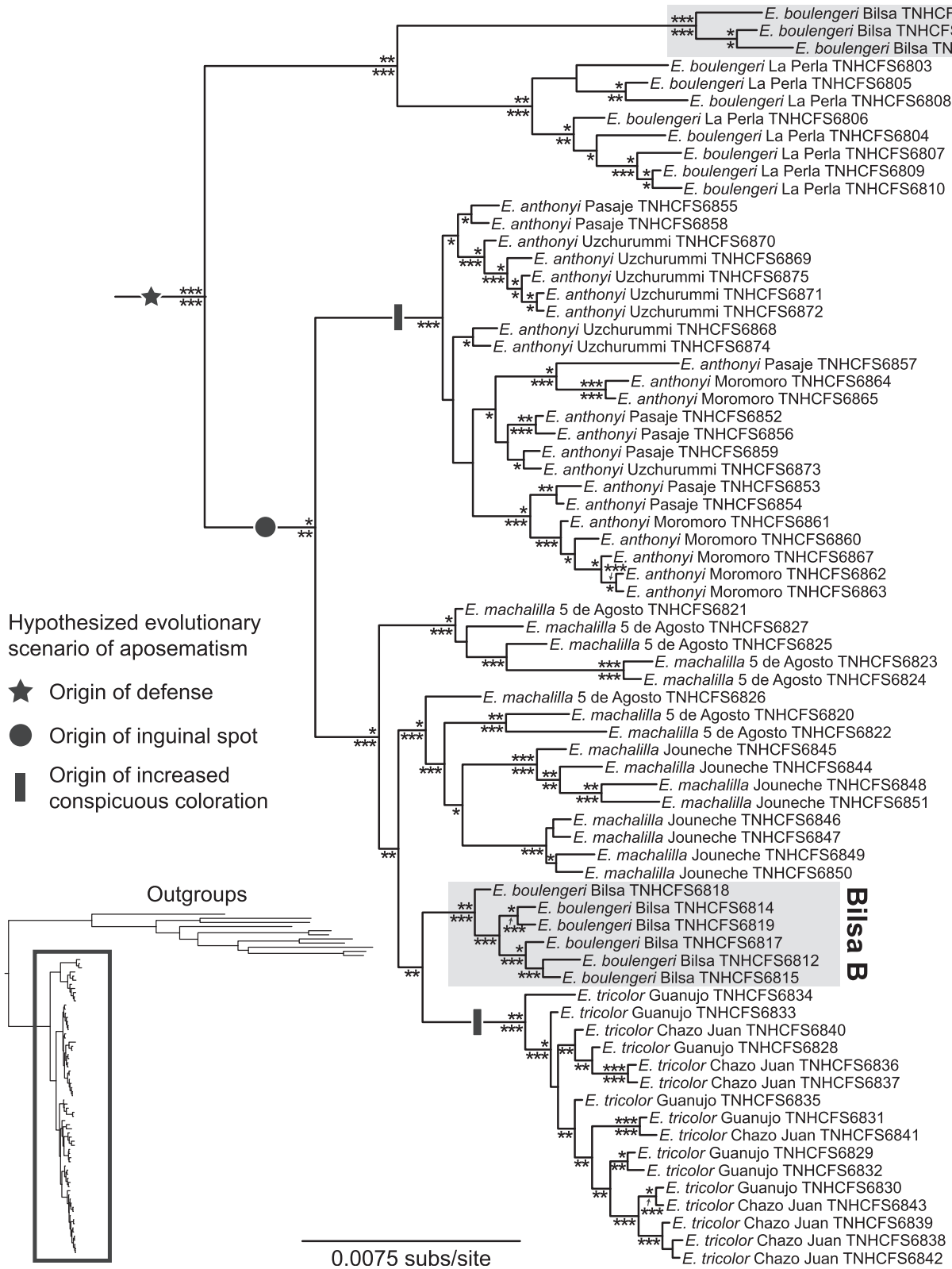


Fig. 2. Bayesian phylogeny of *Epipedobates* based on 12S–16S, *Cytochrome B*, and *Kv1.3*. Individuals are identified by their tissue sample code (TNHCFS series); corresponding specimen voucher numbers (QAZA series) are noted in Supplementary Table S1. Support values for maximum likelihood analysis (1000 bootstraps) are shown above nodes and Bayesian Posterior Probability (bpp) support values are shown below nodes. ***, high support (95–100% bootstrap or 0.95–1.00 bpp); **, moderate support (75–94% bootstrap or 0.75–0.94 bpp); *, low support (50–74% bootstrap or 0.50–0.74 bpp); no stars, very low support (<50% bootstrap or <0.50 bpp). See Supplementary Fig. S1 for maximum likelihood topology. Gray boxes denote the two groups observed in the *E. boulengeri* Bilsa population. Assuming that the anomalous position of Bilsa B is a result of mitochondrial capture (see Section 4.1 in Discussion), the hypothesized evolutionary scenario of aposematism in *Epipedobates* is shown using black symbols.

et al. (2014) for a detailed description of these variables). We also included body size (snout-vent length) and temperature while calling, because they influence spectral (body size-related) and temporal (temperature-related) variables (Wells, 2007). Therefore, for analyses of the acoustic phenotype we used a total of 14 variables.

To quantify differences in call parameters among species, we performed Nonmetric Multidimensional Scaling on the reduced dataset using metaMDS() in the vegan v2.4-1 package in R v3.0.2 (Oksanen et al., 2016). The number of dimensions was set to 2, maximum number of iterations was set to 100, and the dissimilarity index was set to “gower”, which calculates Gower’s distance (Gower, 1971) using both binary and continuous variables.

3. Results

3.1. DNA sequencing

We obtained consensus sequence alignments for a total of 2803 nt: 745 nt of 12S–16S, 691 nt of *Cytochrome B* and 1367 nt of *Kv1.3*. We were unable to sequence 12S–16S for 6 individuals, *Cytochrome B* for 3 individuals, and *Kv1.3* for 4 individuals (Supplementary Table S1). *Kv1.3* contained 49 variable sites of which 33 were parsimony-informative; 12S–16S contained 46 variable sites, of which 36 were parsimony-informative; *Cytochrome B* contained 108 variable sites, of which 93 were parsimony-informative. In addition to these three gene segments, 881 nt of 16S were sequenced for 10 individuals; this gene had 35 variable sites, of which 23 were parsimony-informative.

3.2. Phylogeny estimation

Support for our *Epipedobates* phylogeny (concatenated genes) was moderate to high for the Bayesian tree (Fig. 2) and moderate for the ML tree (Supplementary Fig. S1). All major nodes were concordant between Bayesian and ML trees; there were a few shallow topological differences in the placement of individuals of *E. tricolor* (Chazo Juan population) and *E. machalilla* (Jouneche population), and in branching patterns of populations within *E. anthonyi*. These discrepancies are likely caused by low ML support (<50%) representing equally likely reconstructions of alternative branching patterns at these nodes. In any case, these results do not impact the major conclusions of our paper.

Epipedobates anthonyi and *E. tricolor* formed well-supported clades, but they are not sister-taxa, despite both having conspicuous coloration (Fig. 5; see Results Section 3.5). In both Bayesian and ML analyses, *Epipedobates machalilla* populations did not form a clade; some were closer to *E. tricolor* and to six individuals of *E. boulengeri* (Bilsa B population) than to other *E. machalilla*. However, the node indicating paraphyly of *E. machalilla* is poorly supported; the bootstrap support is <50% and the bpp is <0.95. A deep, strongly supported bifurcation (Fig. 2 and Supplementary Fig. S1) suggests either that *E. boulengeri* represents two distinct lineages (i.e., “cryptic” species), or that there is introgression between *E. boulengeri* and *E. machalilla* (Fig. 3). We were careful to identify individuals of *E. machalilla* and *E. boulengeri* correctly, so we rule out possible misidentifications.

A reference phylogeny of existing *Epipedobates* Genbank sequences (Fig. 1) is largely congruent with our new results. Specifically, in both phylogenies, *E. boulengeri* and *E. machalilla* were recovered as non-monophyletic groups, while *E. tricolor* and *E. anthonyi* were monophyletic. The most noticeable difference between our results (Fig. 2) and the reference phylogeny (Fig. 1) is the position of *E. machalilla* from Manta Real, which in the reference phylogeny was grouped with the *E. anthonyi* clade with very low support (<0.50 bpp).

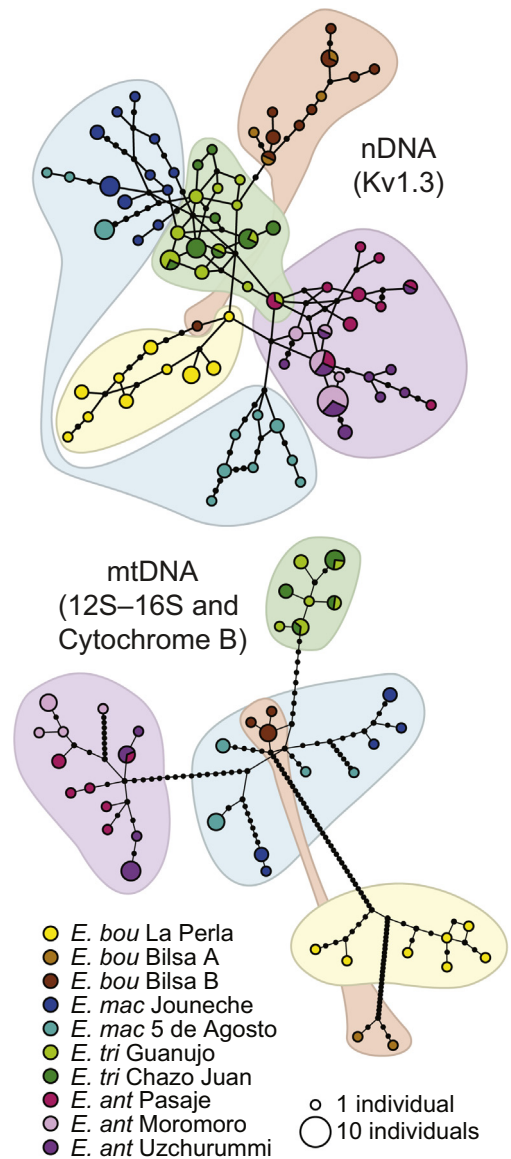


Fig. 3. Haplotype networks estimated in PopART using the Median Joining Network algorithm (Bandelt et al., 1999). Colors represent sampled populations. Filled blobs circumscribe species-level haplotype groups; two blobs are used for *E. boulengeri* Bilsa (brown) and *E. boulengeri* La Perla (yellow) populations to highlight the distinct mtDNA haplotype groups found in this species. *E. bou*, *E. boulengeri*; *E. tri*, *E. tricolor*; *E. ant*, *E. anthonyi*; *E. mac*, *E. machalilla*. (For interpretation of the references to color in this figure legend, the reader is referred to the web version of this article.)

3.3. Pairwise distance and haplotype network analyses

Maximum pairwise divergences (uncorrected-p distances) between individuals pooled across the four species are 3.0% for 12S–16S, 2.6% for 16S, 7.7% for *Cytochrome B*, and 0.4% for *Kv1.3* (Table 1). For both mitochondrial genes the greatest pairwise distance is between individuals of the clade of *E. boulengeri* (La Perla + Bilsa A populations) and individuals from other species (Table 1; Supplementary Tables S4 and S5). Maximum pairwise divergence between populations excluding the *E. boulengeri* clade (La Perla + Bilsa A populations) is 2.0% for 12S–16S, 1.9% for 16S, 4.6% for *Cytochrome B*, and 0.4% for *Kv1.3* (Supplementary Tables S4–S8).

The mtDNA (*Cytochrome B* and 12S–16S) haplotype network indicates that each of the four species of *Epipedobates* has

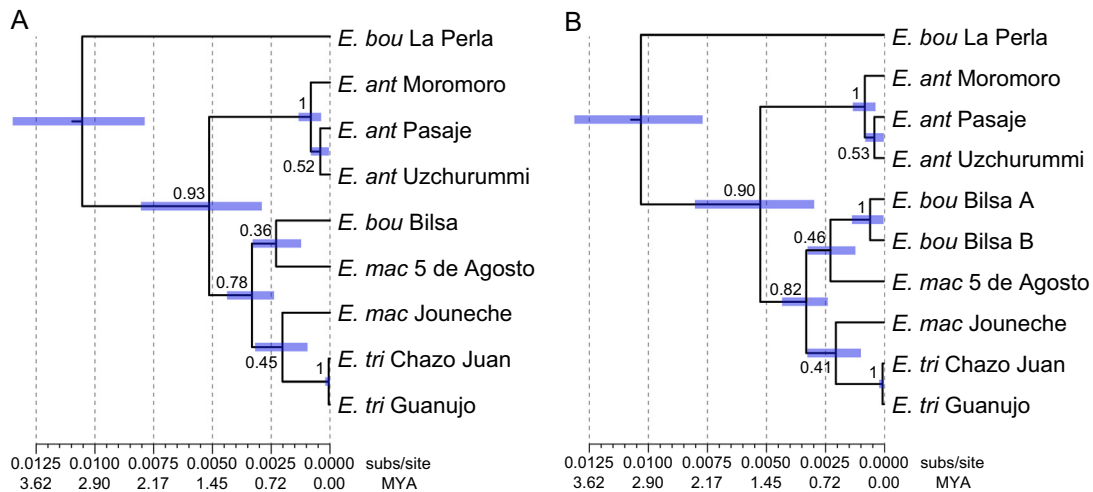


Fig. 4. Maximum clade credibility tree obtained using TreeAnnotator with output from BP&P A01 analyses given (A) nine or (B) ten populations. Node support values are bpps; node bars represent 95% HPD (τ). *E. bou*, *E. bouleengeri*; *E. tri*, *E. tricolor*; *E. ant*, *E. anthonyi*; *E. mac*, *E. machalilla*.

species-specific haplotypes (Fig. 3). The *E. tricolor* and *E. anthonyi* haplotypes (green and purple in Fig. 3) each form clusters separated from haplotypes of the other species by at least nine changes in mtDNA. In contrast, haplotypes of *E. bouleengeri* do not form discrete clusters. Those of Bilsa B (dark brown) are closely connected to those of *E. machalilla* (blue), whereas the haplotypes of *E. bouleengeri* La Perla and Bilsa A (yellow and pale brown) form lineages that are separated by 38 changes from other haplotypes. Therefore, *E. bouleengeri* Bilsa B haplotypes are more similar to *E. machalilla* haplotypes than to other *E. bouleengeri* haplotypes.

The pattern of *Kv1.3* haplotypes is less resolved. Except for one haplotype shared by *E. anthonyi* and *E. tricolor*, each species has unique haplotypes. In contrast to the pattern in mtDNA networks, the *Kv1.3* haplotype clusters of *E. tricolor* and *E. anthonyi* are closely connected by their shared haplotype. The populations of *E. machalilla* (shades of blue in Fig. 3) form two clusters that are separated from each other by seven steps. One *E. machalilla* haplotype cluster is close to *E. tricolor*, but the other (5 de Agosto individuals) is roughly equidistant to haplotypes of *E. bouleengeri* La Perla, *E. anthonyi*, and *E. tricolor*. Finally, while haplotypes of *E. bouleengeri* Bilsa A and Bilsa B form distinct clusters in the mtDNA networks, the *Kv1.3* haplotypes of *E. bouleengeri* Bilsa A and Bilsa B form one cluster, except for one haplotype of one individual (THNCF56818), which was part of the distinct La Perla *E. bouleengeri* haplotype cluster (Fig. 3). Low genetic divergence may have caused this latter pattern.

3.4. Species-tree estimation

All BP&P analyses had acceptable MCMC move proportions (15–70%) and estimated similar τ and θ values, indicating that the analyses likely converged on the most probable model (Supplementary Table S3). We calculated the age (τ) of the root of the clade to be ~ 3 MY and the ancestral effective population size (θ) to be approximately 650,000 individuals (Fig. 4; Supplementary Table S3).

The A11 models (co-estimation of individual assignment and species assignment) strongly supported collapsing *E. tricolor* Chazo Juan (Cha) and Guanujo (Gua) populations into a single putative species ($P[\text{ChaGua}] > 0.966$, Supplementary Table S3). However, there was low support for collapsing *E. bouleengeri* Bilsa populations ($0.500 < P[\text{BilABilB}] < 0.530$, Supplementary Table S3), and no support for collapsing *E. anthonyi* populations ($0.081 < P[\text{MorUzc}] < 0.208$, $0.118 < P[\text{PasUzc}] < 0.164$) or *E. machalilla* populations (see Supplementary Dataset 5). The majority-rule species tree from

A01 models (a priori species assignment; Fig. 4) and the best trees from both A01 and A11 models (Supplementary Table S3) largely matched the ML and Bayesian inference trees (Fig. 2), except that BP&P supported *E. bouleengeri* Bilsa A + Bilsa B populations as sister lineages ($P \approx 1.00$, Fig. 4). Although the posterior probability of the best tree was low in every analysis ($P[\text{Best Tree}] < 0.112$, Supplementary Table S3), the majority-rule consensus trees obtained from A01 models (Fig. 4) strongly supported monophyly of *E. tricolor*, of *E. anthonyi*, and of *E. bouleengeri* Bilsa A + Bilsa B ($P \approx 1.00$). There was moderate support for a clade excluding *E. bouleengeri* La Perla ($0.86 < P < 0.95$, Fig. 4) and for the clade *E. tricolor* + *E. machalilla* + *E. bouleengeri* (Bilsa A + B) ($0.75 < P < 0.84$, Fig. 4). However, BP&P still failed to resolve species-level relationships within this three-species clade.

3.5. Phenotypic analysis

When scaled by maximum pairwise distance, the relative phenotypic divergence better discriminated differences among individuals than the relative genetic divergence (Fig. 5; compare distance along x-axes between nodes in the two dendrograms). *Epipedobates machalilla* and *E. bouleengeri* formed a cluster reflecting their similar dull pattern (cryptic coloration); in contrast, the conspicuously colored *E. anthonyi* and *E. tricolor* did not cluster together and showed the greatest phenotypic distance (Supplementary Table S9). In only one case did an individual cluster with another species: *E. machalilla* (TNHCF56849) was grouped with *E. bouleengeri* Bilsa individuals. Neither dendrogram grouped members of these two species into clusters corresponding to a priori species assignments. However, the genetic distance dendrogram largely recovered the same species-level relationships estimated using Bayesian and ML methods (Figs. 2 and 4).

3.6. Acoustic analysis

In all NMDS runs, minimum stress was < 0.07 (stress ranges from 0 to 1, and values < 0.3 are acceptable), indicating that two dimensions could adequately represent the data. Mating calls of *Epipedobates*, *Silverstoneia*, and *Colostethus* occupied somewhat distinct locations in call parameter space, except for *E. anthonyi*, which fell within the *Silverstoneia* polygon (Fig. 6). In some cases, distance between species of *Epipedobates* was as large as the distance between species of *Silverstoneia* and *Colostethus* (Fig. 6). Thus, the call of each *Epipedobates* species is likely distinct enough to be

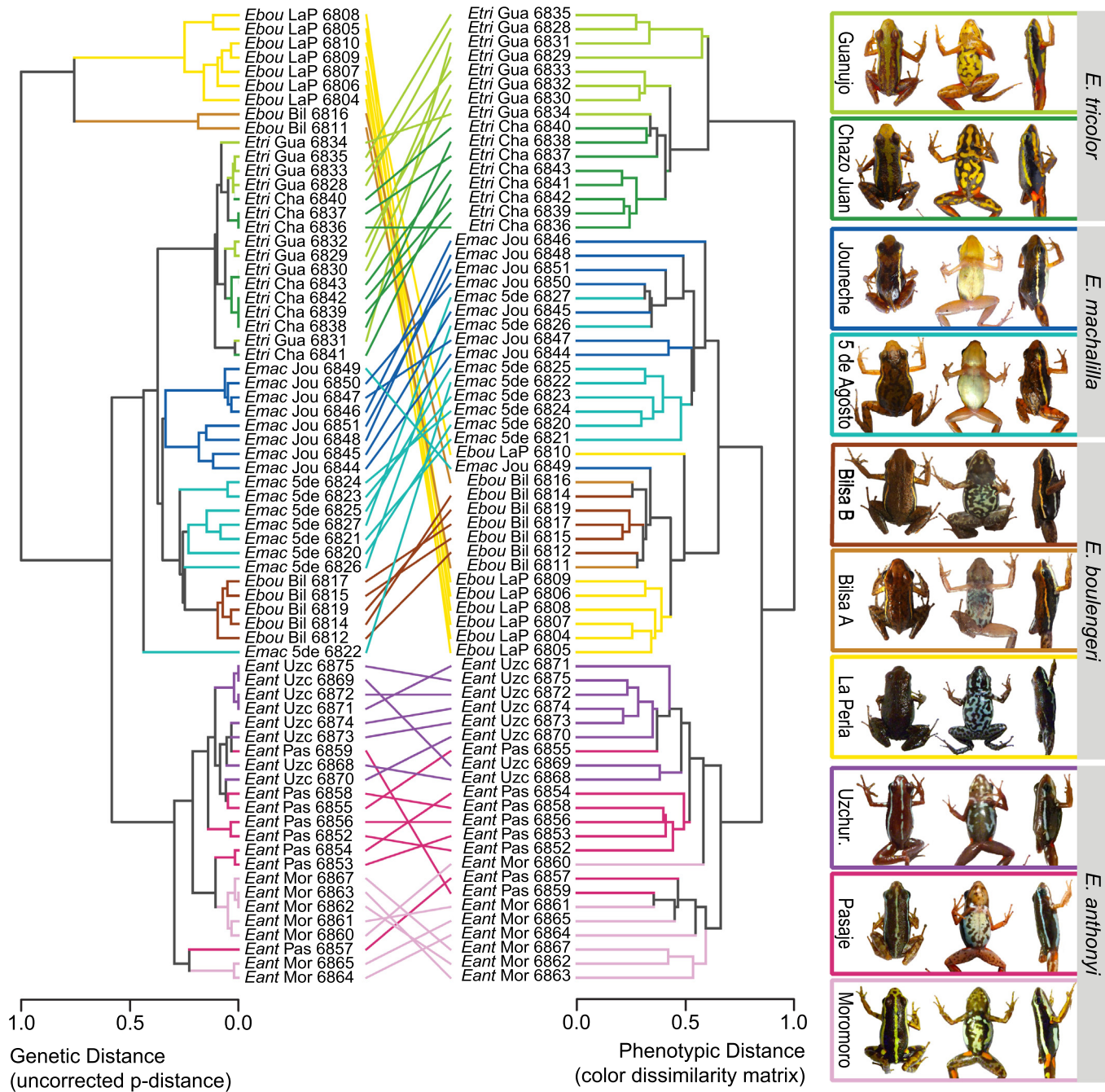


Fig. 5. Dendrograms based on dissimilarity matrices showing relative genetic (concatenated gene matrix) and phenotypic distance. Phenotypic data better recovered population-level species assignments than did genetic data clusters; genetic distance among individuals largely reflected species-level phylogenetic patterns obtained using ML and Bayesian inference. Relative pairwise distances among individuals are much higher in phenotypic than in genetic data. Population abbreviations: Gua, Guanujo; Cha, Chazo Juan; 5de, 5 de Agosto; Bil, Bilsa; Jou, Jouneche; Uzc or Uzchur, Uzchurummi; Pas, Pasaje; Mor, Moromoro; LaP, La Perla. Species abbreviations: *E. ant.*, *E. anthonyi*; *E. mac.*, *E. machalilla*; *E. tri.*, *E. tricolor*; *E. bou.*, *E. boulengeri*. Numbers are TNHCFS tissue sample codes; corresponding specimen voucher numbers (QCAZA series) are noted in [Supplementary Table S1](#).

recognized as heterospecific by other species, suggesting reproductive isolation (Ryan and Rand, 2001).

4. Discussion

4.1. Species-level relationships

The phylogenetic relationships (Fig. 2) largely agree with published phylogenies of *Epipedobates* (Clough and Summers, 2000; Graham et al., 2004; Grant et al., 2006; Santos et al., 2003;

Santos and Cannatella, 2011; Vences et al., 2003). Namely, we found moderate-to-low support for grouping *E. tricolor*, *E. anthonyi*, and *E. machalilla* to the exclusion of *E. boulengeri* (Figs. 1, 2 and 4), with the qualification that some mitochondrial haplotypes of the Bilsa population of *E. boulengeri* grouped with those of *E. machalilla*, likely introduced via introgression. We also found in our reference phylogeny that *E. darwinwallacei* and *E. espinosai* are closer to the *E. machalilla* + *E. tricolor* + *E. anthonyi* clade than to *E. boulengeri* (Fig. 1). However, these two species have restricted ranges, similar calls (Fig. 6), and are poorly sampled, so their validity as species

Table 1

Uncorrected-pairwise distances reveal low genetic diversity within (diagonal) and among (off-diagonal, lower triangle) species of *Epipedobates*. In contrast, there is much greater phenotypic variation within (diagonal, bold) and among *Epipedobates* species (off-diagonal, top triangle, bold). Phenotypic distance was calculated with high-dimensional color and pattern data and standardized by dividing by the maximum distance; see text (Section 2.6) for more information. Each value is shown as mean (range). See Section 2.2 for a description of genes. *cytB*, *Cytochrome B*.

	<i>E. boulengeri</i>	<i>E. machalilla</i>	<i>E. tricolor</i>	<i>E. anthonyi</i>	Sample size
<i>E. boulengeri</i>	0.281 (0.151–0.411) 0.011 (0.000–0.023) 0.041 (0.000–0.068) 0.000 (0.000–0.000) 0.017 (0.009–0.023)	0.461 (0.216–0.695)	0.814 (0.594–1.000)	0.623 (0.458–0.798)	color N = 14 12S–16S N = 16 <i>cytB</i> N = 14 Kv1.3 N = 16 16S N = 3
<i>E. machalilla</i>	0.012 (0.002–0.025) 0.048 (0.006–0.077) 0.001 (0.000–0.003) 0.017 (0.003–0.026)	0.366 (0.213–0.532) 0.004 (0.000–0.010) 0.015 (0.000–0.028) 0.002 (0.000–0.004) 0.014 (NA)	0.718 (0.498–0.910)	0.597 (0.429–0.759)	color N = 16 12S–16S N = 14 <i>cytB</i> N = 16 Kv1.3 N = 16 16S N = 2
<i>E. tricolor</i>	0.016 (0.005–0.027) 0.050 (0.013–0.077) 0.000 (0.000–0.001) 0.013 (0.008–0.018)	0.011 (0.007–0.015) 0.021 (0.015–0.031) 0.001 (0.000–0.004) 0.008 (0.004–0.013)	0.340 (0.149–0.516) 0.002 (0.000–0.003) 0.003 (0.000–0.006) 0.001 (0.000–0.001) 0.003 (NA)	0.656 (0.416–0.917)	color N = 16 12S–16S N = 15 <i>cytB</i> N = 16 Kv1.3 N = 15 16S N = 2
<i>E. anthonyi</i>	0.016 (0.008–0.030) 0.055 (0.026–0.077) 0.000 (0.000–0.000) 0.020 (0.015–0.026)	0.010 (0.007–0.020) 0.034 (0.024–0.046) 0.001 (0.000–0.003) 0.015 (0.012–0.019)	0.015 (0.013–0.020) 0.038 (0.033–0.044) 0.000 (0.000–0.001) 0.010 (0.008–0.012)	0.411 (0.153–0.698) 0.001 (0.000–0.008) 0.010 (0.000–0.020) 0.000 (0.000–0.000) 0.004 (0.004–0.005)	color N = 23 12S–16S N = 21 <i>cytB</i> N = 23 Kv1.3 N = 21 16S N = 3

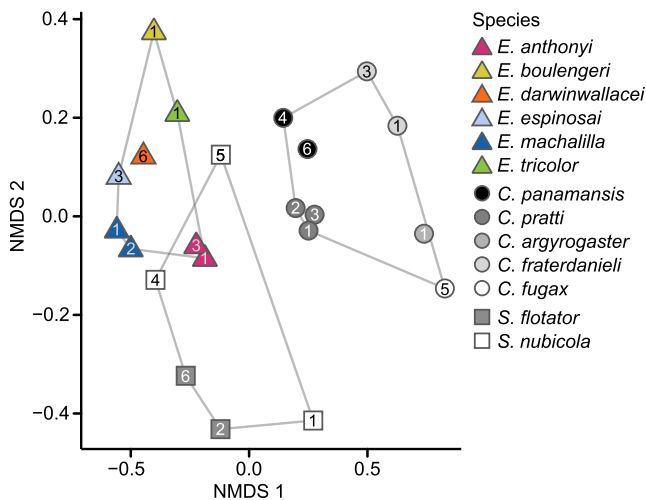


Fig. 6. Non-metric multidimensional scaling of acoustic variation in *Epipedobates* and two closely related poison frog taxa, *Colostethus* and *Silverstoneia*. Polygons delineate acoustic space for each genus. Call variation within *Epipedobates* is nearly as high as within the other two genera; some, but not all, *Epipedobates* species are as different from each other as species from two different genera. Data were obtained from Supplementary Table S1 in Santos et al. (2014). Number of males recorded per population is indicated within each symbol. Sound recordings are deposited at the Cornell Lab of Ornithology's Macaulay Library (accession ACC3643; see Supplementary Table S10).

warrants further investigation. The relationships among *E. tricolor*, *E. anthonyi*, and *E. machalilla* could not be resolved unambiguously, likely because of incomplete lineage sorting (ILS), mitochondrial capture, and/or few informative characters, which are all common in very recent speciation events. We explain patterns that may have contributed to *Epipedobates* speciation and then describe the early steps of phylogenetic and phenotypic divergence associated with the origin of aposematism in *Epipedobates*.

Firstly, we found that individuals of *E. tricolor* are nested within *E. machalilla* in all genetic analyses (Figs. 1, 2 and 5). In addition, the haplotypes of *E. machalilla* are similar to those of *E. tricolor* in both gene networks (Fig. 3). These species occupy different environmental niches, with *E. machalilla* inhabiting warmer and drier

habitats at lower elevations than *E. tricolor* (Graham et al., 2004). The distribution of *E. tricolor* is rather small (<5000 km²; Graham et al., 2004), restricted mostly to foothills in central Ecuador, and is parapatric to *E. machalilla* (Fig. 1). These patterns suggest that *E. tricolor* diverged recently from *E. machalilla* (e.g., in the Pleistocene less than 2 MYA; see Fig. 4 and Santos et al., 2009), and that ecological and phenotypic divergence has potentially occurred at a faster rate than genetic divergence. Thus, *E. tricolor* likely represents either a case of speciation by peripheral isolation, or a highly phenotypically divergent population of *E. machalilla* (see Figs. 5 and 6). In both cases, ILS of gene trees can cause a putative species lineage to appear nested within another species lineage in a species tree (Chen et al., 2009; Foote, 1996). This pattern, which we observe (Fig. 2), is not unexpected given the young origin of the clade (Pamilo and Nei, 1988; Santos et al., 2009).

Secondly, our data suggest that mitochondrial capture has happened at least once in *Epipedobates*, specifically from *E. machalilla* into *E. boulengeri* from Bilsa. Our results show disparate phylogenetic placements and deep divergence of the two *E. boulengeri* clusters, consistent with the introgression of alleles from another species into *E. boulengeri* (Figs. 2 and 4). This interpretation is supported by the mtDNA haplotype network, which shows that *E. boulengeri* Bilsa B haplotypes are more similar to *E. machalilla* than to *E. boulengeri* Bilsa A (Fig. 3), and therefore it is likely that Bilsa B mitochondria were captured from an *E. machalilla* population.

In contrast, the nDNA haplotype network clusters *E. boulengeri* Bilsa A and B individuals together (with one exception, a haplotype of Bilsa B individual TNHCF56818 that groups with the La Perla cluster; Fig. 3). Likewise, our BP&P analyses also favor monophyly of *E. boulengeri* Bilsa A + Bilsa B individuals (Fig. 4B); however, the analyses retain a deep split between La Perla and Bilsa, perhaps owing to the strong *machalilla*-like signal from Bilsa B individuals (Fig. 2). The habitats of *Epipedobates machalilla* and *E. boulengeri* are similar (Graham et al., 2004), and the Bilsa *E. boulengeri* population is near the distributional edge of *E. boulengeri* and *E. machalilla* (Fig. 1), so gene flow between species at some point in the past is likely.

Thirdly, we expected that BP&P would resolve a species tree for *Epipedobates*, but it did not (Fig. 4). Perhaps the foremost reason for this failure is lack of informative sites. Although MSC methods are

claimed to perform well with few loci as long as there are sufficient individuals (Zhang et al., 2011), our *Kv1.3* data has relatively few variable sites. The placement of *E. boulengeri* within the *E. machalilla* + *E. tricolor* clade is probably an artifact of introgression between *E. boulengeri* and *E. machalilla* because most MSCs assume that gene-tree discordance is a result of ILS rather than introgression (Camargo et al., 2012a; Carstens et al., 2013; Yang and Rannala, 2010). Although MSCs have been shown to perform adequately with <0.1 migrants per generation (Camargo et al., 2012b; Zhang et al., 2011), an intermediate rate of migration will yield low support and a potentially misleading species tree (Yang, 2015a). In addition, MSCs rely on identifying a gap between the timing of allele coalescence among different lineages to delimit species, and when species rapidly diverge, these gaps are difficult to identify (Camargo et al., 2012b; Reid and Carstens, 2012). Moreover, with few loci and short divergence times (as in our study), BP&P has been shown to have only 65% accuracy in its ability to delimit species (Camargo et al., 2012b). Migration among populations lowers this accuracy to only 50% (Camargo et al., 2012b).

We suggest that BP&P overestimated the number of species in this clade, as it only provided high support for collapsing the two *E. tricolor* populations, which were by far the geographically closest and genetically similar populations of any species (Fig. 1, Table 1). Surprisingly, BP&P did not combine the three populations of *E. anthonyi*, which were highly supported as a clade by our analyses (Figs. 2, 4 and 5; Supplementary Table S3). Although our data may not contain the information necessary for BP&P to delimit species or infer species-level relationships, they do suggest a complex pattern of two widespread, less conspicuous phenotypes (*E. boulengeri* and *E. machalilla*) with narrowly distributed, apparently independently derived and conspicuous phenotypes (*E. tricolor* and *E. anthonyi*). We suggest that genomic approaches such as RADseq are necessary to provide sufficient data to resolve patterns of divergence within *Epipedobates*.

The age of the *Epipedobates* clade predicted by BP&P, ~3 MY, is younger than that estimated by Santos et al. (2009), ~5 MY. This may be in part because Santos and colleagues used an *E. boulengeri* specimen from Isla Gorgona, Colombia, which is the oldest lineage of the clade (Fig. 1, *E. boulengeri* Gorgona specimen) and is fairly divergent from the Ecuadorian samples of *E. boulengeri* that we included (i.e., populations close to the *E. boulengeri* Durango specimen in Fig. 1). In addition, differences in estimated mutation rates used to convert the units of the τ parameter could have altered the estimated divergence times. Unfortunately, without independent calibrations within Dendrobatidae it is difficult to evaluate the accuracy of our estimates. Nevertheless, *Epipedobates* remains the youngest aposematic clade of dendrobatid poison frogs with any of these estimates.

4.2. Genetic versus phenotypic and acoustic divergence

Genetic divergence across *Epipedobates* species was low (Table 1) in contrast with their substantial interspecific phenotypic and acoustic variation (Table 1, Figs. 5 and 6; Santos et al., 2014; Tarvin et al., in review). *Epipedobates anthonyi* and *E. tricolor* are aposematic, and even the more inconspicuous *E. boulengeri* has a vividly patterned venter that is lacking in *E. machalilla* (Fig. 5). Not only are these species phenotypically distinct, they also differ in environmental niche (Graham et al., 2004), and possess mating calls that are likely different enough to act as prezygotic isolating mechanisms (Fig. 6) (Santos et al., 2014). Acoustic divergence in courtship signal has long been associated with speciation in birds, anurans, and insects (Blair, 1955; Edwards et al., 2005; Gerhardt and Huber, 2002; Ryan and Rand, 2001); hence, divergence in mating calls of *Epipedobates* species supports distinctiveness of the species (Guarnizo et al., 2012; Guerra and Ron, 2008). We note

however, that our sample is limited, and that lower divergence may be found in other populations, particularly where introgression has occurred. In addition, we highlight that *E. darwinwallacei* and *E. espinosai* do not differ substantially in acoustic parameters; genetic information will help resolve their status as species.

Within aposematic poison frogs, high phenotypic variation despite low genetic divergence is not uncommon. Some clades within *Dendrobates* and *Ameerega* have average interspecific pairwise divergences <2.0% (16S) comparable to *Epipedobates* (Brusa et al., 2013; Fouquet et al., 2007; Jansen et al., 2011; Perez-Peña et al., 2010; Wang, 2011; Wang and Shaffer, 2008) (Table 1). However, within *Dendrobates* (*Oophaga*) *pumilio*, a species with unparalleled interpopulation divergence in color and pattern, the greatest divergence in *Cytochrome B* p-distance among the Bocas del Toro Archipelago populations (250 km²) was 6.8% (Hauswaldt et al., 2011), compared with 7.7% p-distance in *Cytochrome B* across the four species of *Epipedobates*. Consequently, if the same criteria used to define the polymorphic *D. (O.) pumilio* lineage as one species are applied to *Epipedobates*, then all nominal species within *Epipedobates* should be considered morphs of the first described species in the genus, *Epipedobates anthonyi* (Noble, 1921). We open this discussion to further investigation.

In contrast, taxonomic reviews of other Neotropical frogs are plagued with examples of the opposite pattern, the paradigm of “cryptic” species—genetically divergent, closely related species that are almost indistinguishable morphologically (e.g., Elmer et al., 2013; Fouquet et al., 2016; Funk et al., 2012; Ortega-Andrade et al., 2015; Padial and De La Riva, 2009). *Epipedobates* differs from most of these examples in being aposematic, which might explain the unusual combination of low genetic and high morphological divergence. Aposematism is correlated with increased rates of speciation in dendrobatids (Santos et al., 2014) and generally in other taxa (Przezcak et al., 2008), and thus young clades of aposematic poison frogs may have low genetic divergence despite being independent lineages. How to delimit species in such cases is not clear, and an overestimate of the number of species is likely, especially if species descriptions rely largely on coloration and one or two molecular markers. Likewise, species identification based on DNA barcoding (Hebert et al., 2004) may also be unreliable because it will not discern species that are weakly diverged genetically or resolve species that have captured mtDNA of another species, as in our *E. boulengeri* Bilsa B population. Multiple sources of data (e.g., species distribution modeling, acoustic characterization, morphometrics, and genomic characterization, considered in the context of “integrative taxonomy”) will be necessary for effective species delimitation in aposematic organisms.

4.3. The early stages of the evolution of aposematism in *Epipedobates*

Aposematism in poison frogs (Dendrobatidae) is a complex trait that integrates evolution in diet (the source of defensive alkaloids), physiology, behavior, morphology, and other traits (Santos and Cannatella, 2011). Its evolution can be represented simplistically as a series of stepwise changes, the precise order of which remains unknown (Santos and Cannatella, 2011). However, a likely scenario is that increased consumption of defended arthropods (diet specialization) evolved first, selecting for resistance to alkaloids and favoring either delayed excretion or active sequestration of alkaloids. These processes would have produced a progressive bioaccumulation of noxious (or at least distasteful) substances, which would have provided defense against predators and a survival advantage. Lastly, bright coloration (i.e., warning signals) likely evolved in the frogs as a warning of their chemical defenses to their enemies (Darst and Cummings, 2006; Santos et al., 2016). Such a scenario has been observed in Cuban frogs of the genus *Eleutherodactylus* (Rodríguez et al., 2013). In this lineage, sequestration

preceded the evolution of warning signals, and increased sequestration is associated with more conspicuous warning signals, which appear strikingly similar to those of *Epipedobates*. These observations support long-held assumptions regarding origins of aposematism, i.e., that warning signals arise from within cryptic and defended populations (Sillen-Tullberg and Bryant, 1983). Although diet in the *Eleutherodactylus limbatus* group has not been studied, Rodríguez and colleagues hypothesized that because body size became smaller during the evolution of defense, their diet may also have changed to include smaller prey items such as those consumed by defended dendrobatids.

Although *Epipedobates* is the smallest and youngest of the aposematic clades (~7 species and ~5 MY old compared to *Dendrobates* + *Phyllobates*: ~50 species, ~30 MY old, and *Ameerega*: ~30 species, ~10 MY old), it presents the greatest interspecific variation across the extremes of aposematic phenotype (inconspicuous to conspicuous, undefended to defended), offering a glimpse of the early stages of the evolution of aposematism (Santos et al., 2016). A core component of aposematism in poison frogs is alkaloid defense. Purportedly, all species of *Epipedobates* except *E. machalilla* have alkaloids (Cipriani and Rivera, 2009; Daly et al., 1987; Santos and Cannatella, 2011), and alkaloids have not been found in the clade sister to *Epipedobates*, *Silverstoneia*, although not all species of *Silverstoneia* have been surveyed (Daly et al., 1987; Poulin et al., 2001). From this we infer that some components of aposematism (diet specialization, alkaloid resistance, and alkaloid sequestration) evolved at the base of the *Epipedobates* clade and may have been lost in *E. machalilla* (Santos and Cannatella, 2011) (Fig. 2). Nevertheless, only one population of *E. machalilla* (Rio Ayampe, Ecuador) has been tested for alkaloids, using a coarse technique (Santos and Cannatella, 2011). Because poison frog defenses are known to vary substantially across populations and time (Cipriani and Rivera, 2009; McGugan et al., 2016; Saporito et al., 2012, 2007) and reversals of the aposematic phenotype are rare in Dendrobatidae (Santos et al., 2014), it is possible that some populations of *E. machalilla* are chemically defended. Considering the physiological changes necessary for alkaloid defenses (Santos et al., 2016; Tarvin et al., 2016) and possible gene flow between *E. machalilla* and the defended *E. boulengeri*, we suspect that further analyses of *E. machalilla* will reveal some level of defense.

The warning component of aposematism in poison frogs is conspicuous coloration. In our phenotypic analyses, the phenotypic differences between *E. machalilla* and *E. boulengeri* are slight, whereas the two most conspicuous species *E. tricolor* and *E. anthonyi* form separate, well-defined clusters (Fig. 5). Because the most recent common ancestor of *Epipedobates* was likely inconspicuous (i.e., similar in color and pattern to *E. boulengeri*; see Fig. 1), this result supports the phylogenetic pattern of two independent origins of conspicuous phenotypes in *E. tricolor* and *E. anthonyi*. There is an equally parsimonious explanation if one considers only a simplistic loss/gain of character states: one origin of conspicuous coloration in the ancestor of the *E. anthonyi* + *E. machalilla* + *E. tricolor* clade plus a reversal of the conspicuous coloration in *E. machalilla*; however, this seems unlikely if *E. machalilla* is not monophyletic, because multiple reversals would be required. Because the phylogenetic positions of *E. darwinwallacei* (conspicuous, defended), *E. narinensis* (possibly conspicuous, defense unknown), and *E. espinosai* (inconspicuous, defended) are not fully resolved, we cannot determine whether *E. darwinwallacei* represents a third origin of aposematism, or if it shares a common origin with the *E. anthonyi* + *E. machalilla* + *E. tricolor* clade.

Interestingly, *E. machalilla*, *E. anthonyi*, and *E. tricolor* all possess red or orange inguinal flash marks that are absent in *E. boulengeri*, *E. darwinwallacei*, *E. narinensis*, and *E. espinosai* (Figs. 1 and 5; Coloma, 1995). Such patches are thought to disrupt search images

of a hunting predator or to signal anti-predator defenses (Edmunds, 1974; Toledo and Haddad, 2009). Hence, we find evidence supporting one origin of some components of warning coloration in the ancestor of *E. anthonyi* + *E. machalilla* + *E. tricolor*, with an overall increase in conspicuousness in *E. tricolor* and *E. anthonyi* (Fig. 2). These latter two species may be the most highly defended of the genus in alkaloid diversity and quantity (Cipriani and Rivera, 2009; Tarvin et al., 2016); if true, an increase in conspicuousness in these two lineages is not an unexpected consequence.

We caution that the efficacy of coloration and alkaloid defense has not been tested experimentally in any species of *Epipedobates*. Our scenario derives from work by Darst et al. (2006), who showed that for three species of *Ameerega* (*A. hahneli*, *A. parvula*, and *A. bilinguis*; formerly *Epipedobates*), conspicuousness in color and alkaloid load were strongly related, and furthermore, predators learned more quickly to avoid bright, toxic species over inconspicuous and more palatable species. In *Ameerega*, the greatest p-distance in *Cytochrome B* among the three species is 13.5%, in contrast to the 7.7% in *Epipedobates* (our analysis of data from Santos and Cannatella, 2011); thus *Epipedobates* may represent an early stage in the evolution of aposematic syndrome. Parallel studies of predator-prey interactions in *Epipedobates* would provide a valuable and phylogenetically relevant comparison.

Acknowledgments

This project was funded in part by the University of Texas at Austin through an Ecology, Evolution, and Behavior Graduate Research Grant to RDT, an Undergraduate Research Grant to EAP, and by NSF 1556967 to DCC. Fieldwork was also supported by grants from the Society of Systematic Biologists, North Carolina Herpetological Society, Society for the Study of Reptiles and Amphibians, Chicago Herpetological Society, and the Texas Herpetological Society to RDT. RDT was supported by the National Science Foundation Graduate Research Fellowship Program. We thank field assistants Cristina Toapanta and Nick Jones for their assistance in specimen collection, Travis LaDuc of the Biodiversity Collections of the Department of Integrative Biology for assistance with providing specimen records, and the Ecuadorian Ministry of the Environment for their help in facilitating specimen collection. JCS thanks Jack W. Sites Jr. for his support at Brigham Young University. SRR thanks SENESCYT, Arca de Noe program, for its support of specimen and tissue collections at QCAZ.

Appendix A. Supplementary material

Supplementary data associated with this article can be found, in the online version, at <http://dx.doi.org/10.1016/j.ympbev.2016.12.035>.

References

- Bandelt, H.J., Forster, P., Röhl, A., 1999. Median-joining networks for inferring intraspecific phylogenies. *Mol. Biol. Evol.* 16, 37–48. <http://dx.doi.org/10.1093/oxfordjournals.molbev.a026036>.
- Blair, W.F., 1955. Mating call and stage of speciation in the *Microhyala olivacea*-*M. carolinensis* complex. *Evolution* 9, 469–480. <http://dx.doi.org/10.2307/2405481>.
- Brusa, O., Bellati, A., Meuche, I., Mundy, N.J., Pröhl, H., 2013. Divergent evolution in the polymorphic granular poison-dart frog, *Oophaga granulifera*: genetics, coloration, advertisement calls and morphology. *J. Biogeogr.* 40, 394–408. <http://dx.doi.org/10.1111/j.1365-2699.2012.02786.x>.
- Camargo, A., Avila, L.J., Morando, M., Sites, J.W., 2012a. Accuracy and precision of species trees: effects of locus, individual, and base pair sampling on inference of species trees in lizards of the *Liolaemus darwini* group (Squamata, Liolaemidae). *Syst. Biol.* 61, 272–288. <http://dx.doi.org/10.1093/sysbio/syr105>.
- Camargo, A., Morando, M., Avila, L.J., Sites, J.W., 2012b. Species delimitation with ABC and other coalescent-based methods: a test of accuracy with simulations and an empirical example with lizards of the *Liolaemus darwini* complex

- (Squamata: Liolaemidae). *Evolution* 66, 2834–2849. <http://dx.doi.org/10.5061/dryad.4409k652>.
- Carstens, B.C., Pelletier, T.A., Reid, N.M., Satler, J.D., 2013. How to fail at species delimitation. *Mol. Ecol.* 22, 4369–4383. <http://dx.doi.org/10.1111/mec.12413>.
- Castresana, J., 2000. Selection of conserved blocks from multiple alignments for their use in phylogenetic analysis. *Mol. Biol. Evol.* 17, 540–552. <http://dx.doi.org/10.1093/oxfordjournals.molbev.a026334>.
- Chen, W., Bi, K., Fu, J., 2009. Frequent mitochondrial gene introgression among high elevation Tibetan megophryid frogs revealed by conflicting gene genealogies. *Mol. Ecol.* 18, 2856–2876. <http://dx.doi.org/10.1111/j.1365-294X.2009.04258.x>.
- Cipriani, I., Rivera, M., 2009. Detección de alcaloides en la piel de cuatro especies de anfibios ecuatorianos (Anura: Dendrobatidae). *Rev. Ecuat. Med. Cienc. Biol.* 30, 42–49.
- Cisneros-Heredia, D.F., Yáñez-Muñoz, M.H., 2010. A new poison frog of the genus *Epiplatobates* (Dendrobatoidea: Dendrobatidae) from the north-western Andes of Ecuador. *Am. Ciencias Ing.* 2, B83–B86.
- Clough, M.E., Summers, K., 2000. Phylogenetic systematics and biogeography of the poison frogs: evidence from mitochondrial DNA sequences. *Biol. J. Linn. Soc.* 70, 515. <http://dx.doi.org/10.1111/j.1095-8312.2000.tb01236.x>.
- Coloma, L.A., 1995. Ecuadorian frogs of the genus *Colostethus* (Anura: Dendrobatidae). *Misc. Publ. Univ. Kansas Museum Nat. Hist.* 87, 1–72.
- Cummings, M.E., Crothers, L.R., 2013. Interacting selection diversifies warning signals in a polytypic frog: an examination with the strawberry poison frog. *Ecol. Evol.* 27, 693–710. <http://dx.doi.org/10.1007/s10682-013-9648-9>.
- Daly, J.W., Myers, C.W., Whittaker, N., 1987. Further classification of skin alkaloids from neotropical poison frogs (Dendrobatidae), with a general survey of toxic/noxious substances in the Amphibia. *Toxicol.* 25, 1023–1095. [http://dx.doi.org/10.1016/0378-8741\(88\)90060-8](http://dx.doi.org/10.1016/0378-8741(88)90060-8).
- Darriba, D., Taboada, G.L., Doallo, R., Posada, D., 2012. JModelTest 2: more models, new heuristics and parallel computing. *Nat. Methods* 9. <http://dx.doi.org/10.1038/nmeth.2109>. 772–772.
- Darst, C.R., Cummings, M.E., 2006. Predator learning favours mimicry of a less-toxic model in poison frogs. *Nature* 440, 208–211. <http://dx.doi.org/10.1038/nature04297>.
- Darst, C.R., Cummings, M.E., Cannatella, D.C., 2006. A mechanism for diversity in warning signals: conspicuousness versus toxicity in poison frogs. *Proc. Natl. Acad. Sci. USA* 103, 5852–5857. <http://dx.doi.org/10.1073/pnas.0600625103>.
- Dayrat, B., 2005. Towards integrative taxonomy. *Biol. J. Linn. Soc.* 85, 407–415.
- de Queiroz, K., 2007. Species concepts and species delimitation. *Syst. Bot.* 56, 879–886. <http://dx.doi.org/10.1080/10635150701701083>.
- de Queiroz, K., 2005. Different species problems and their resolution. *BioEssays*. <http://dx.doi.org/10.1002/bies.20325>.
- Drummond, A.J., Suchard, M.A., Xie, D., Rambaut, A., 2012. Bayesian Phylogenetics with BEAUti and the BEAST 1.7. *Mol. Biol. Evol.* 29, 1969–1973. <http://dx.doi.org/10.1093/molbev/mss075>.
- Edgar, R.C., 2004. MUSCLE: multiple sequence alignment with high accuracy and high throughput. *Nucl. Acids Res.* 32, 1792–1797. <http://dx.doi.org/10.1093/nar/gkh340>.
- Edmunds, M., 1974. *Defence in Animals: A Survey of Anti-Predator Defences*. Longman, New York.
- Edwards, S.V., Kingan, S.B., Calkins, J.D., Balakrishnan, C.N., Jennings, W.B., Swanson, W.J., Sorenson, M.D., 2005. Speciation in birds: genes, geography, and sexual selection. *Proc. Natl. Acad. Sci. USA* 102 (Suppl.), 6550–6557. <http://dx.doi.org/10.1073/pnas.0501846102>.
- Elmer, K.R., Bonett, R.M., Wake, D.B., Lougheed, S.C., 2013. Early Miocene origin and cryptic diversification of South American salamanders. *BMC Evol. Biol.* 13, 59. <http://dx.doi.org/10.1186/1471-2148-13-59>.
- Endler, J.A., 2012. A framework for analysing colour pattern geometry: adjacent colours. *Biol. J. Linn. Soc.* 107, 233–253. <http://dx.doi.org/10.1111/j.1095-8312.2012.01937.x>.
- Foote, M., 1996. On the probability of ancestors in the fossil record. *Paleobiology* 22, 141–151.
- Fouquet, A., Gilles, A., Vences, M., Marty, C., Blanc, M., Gemmill, N.J., 2007. Underestimation of species richness in neotropical frogs revealed by mtDNA analyses. *PLoS ONE* 2, e1109. <http://dx.doi.org/10.1371/journal.pone.0001109>.
- Fouquet, A., Martinez, Q., Zeidler, L., Courtois, E.A., Gaucher, P., Blanc, M., Lima, J.D., Souza, S.M., Rodrigues, M.T., Kok, P.J.R., 2016. Cryptic diversity in the *Hypsiboas semilineatus* species group (Amphibia, Anura) with the description of a new species from the eastern Guiana Shield. *Zootaxa* 4084, 79–104. <http://dx.doi.org/10.11646/zootaxa.4084.1.3>.
- Fujita, M.K., Leaché, A.D., Burbrink, F.T., McGuire, J.A., Moritz, C., 2012. Coalescent-based species delimitation in an integrative taxonomy. *Trends Ecol. Evol.* 27, 480–488. <http://dx.doi.org/10.1016/j.tree.2012.04.012>.
- Funk, W.C., Caminer, M., Ron, S.R., 2012. High levels of cryptic species diversity uncovered in Amazonian frogs. *Proc. R. Soc. B Biol. Sci.* 279, 1806–1814. <http://dx.doi.org/10.1098/rspb.2011.1653>.
- Galili, T., 2015. Dendextend: an R package for visualizing, adjusting and comparing trees of hierarchical clustering. *Bioinformatics* 31, 3718–3720. <http://dx.doi.org/10.1093/bioinformatics/btv428>.
- Gerhardt, H.C., Huber, F., 2002. *Acoustic Communication in Insects and Anurans: Common Problems and Diverse Solutions*. University of Chicago Press, Chicago.
- Goebel, A.M., Donnelly, J.M., Atz, M.E., 1999. PCR primers and amplification methods for 12S ribosomal DNA, the control region, Cytochrome Oxidase I, and Cytochrome B in bufonids and other frogs, and an overview of PCR primers which have amplified DNA in amphibians successfully. *Mol. Phylogenet. Evol.* 11, 163–199. <http://dx.doi.org/10.1006/mpev.1998.0538>.
- Gower, J.C., 1971. A general coefficient of similarity and some of its properties. *Biometrics* 27, 857–871. <http://dx.doi.org/10.2307/2528823>.
- Graham, C.H., Ron, S.R., Santos, J.C., Schneider, C.J., Moritz, C., 2004. Integrating phylogenetics and environmental niche models to explore speciation mechanisms in dendrobatid frogs. *Evolution* 58, 1781–1793. <http://dx.doi.org/10.1111/j.0014-3820.2004.tb00461.x>.
- Grant, T., Frost, D.R., Caldwell, J.P., Gagliardo, R., Haddad, C.F.B., Kok, P.J.R., Means, D. B., Noonan, B.P., Schargel, W.E., Wheeler, W.C., 2006. Phylogenetic systematics of dart-poison frogs and their relatives (Amphibia: Athesphatanura: Dendrobatidae). *Bull. Am. Museum Nat. Hist.* 299, 1–262. [http://dx.doi.org/10.1206/0003-0090\(2006\)299\[1:PSODFA\]2.0.CO;2](http://dx.doi.org/10.1206/0003-0090(2006)299[1:PSODFA]2.0.CO;2).
- Guarnizo, C.E., Escallón, C., Cannatella, D., Amézquita, A., 2012. Congruence between acoustic traits and genealogical history reveals a new species of *Dendropsophus* (Anura: Hylidae) in the high Andes of Colombia. *Herpetologica* 68, 523–540. <http://dx.doi.org/10.1655/HERPETOLOGICA-D-10-00038>.
- Guerra, M.A., Ron, S.R., 2008. Mate choice and courtship signal differentiation promotes speciation in an Amazonian frog. *Behav. Ecol.* 19, 1128–1135. <http://dx.doi.org/10.1093/beheco/arn098>.
- Hauswaldt, J.S., Ludewig, A.K., Vences, M., Pröhl, H., 2011. Widespread co-occurrence of divergent mitochondrial haplotype lineages in a Central American species of poison frog (*Oophaga pumilio*). *J. Biogeogr.* 38, 711–726. <http://dx.doi.org/10.1111/j.1365-2699.2010.02438.x>.
- Hebert, P.D.N., Stoeckle, M.Y., Zemlak, T.S., Francis, C.M., 2004. Identification of birds through DNA barcodes. *PLoS Biol.* 2. <http://dx.doi.org/10.1371/journal.pbio.0020312>.
- Jansen, M., Bloch, R., Schulze, A., Pfenninger, M., 2011. Integrative inventory of Bolivia's lowland anurans reveals hidden diversity. *Zool. Scr.* 40, 567–583. <http://dx.doi.org/10.1111/j.1463-6409.2011.00498.x>.
- Knowles, L.L., Carstens, B.C., 2007. Delimiting species without monophyletic gene trees. *Syst. Biol.* 56, 887–895. <http://dx.doi.org/10.1080/10635150701701091>.
- Kumar, S., Nei, M., Dudley, J., Tamura, K., 2008. MEGA: A biologist-centric software for evolutionary analysis of DNA and protein sequences. *Brief. Bioinform.* 9, 299–306. <http://dx.doi.org/10.1093/bib/bbn017>.
- Librado, P., Rozas, J., 2009. DnaSP v5: A software for comprehensive analysis of DNA polymorphism data. *Bioinformatics* 25, 1451–1452. <http://dx.doi.org/10.1093/bioinformatics/btp187>.
- Maddison, W.P., Maddison, D.R., 2015. Mesquite: a modular system for evolutionary analysis. Version 3.04. <http://mesquiteproject.org/wikipaces.com>.
- Marshall, D.C., 2010. Cryptic failure of partitioned bayesian phylogenetic analyses: lost in the land of long trees. *Syst. Biol.* 59, 108–117. <http://dx.doi.org/10.1093/sysbio/syp080>.
- McGugan, J.R., Byrd, G.D., Roland, A.B., Caty, S.N., Kabir, N., Tapia, E.E., Trauger, S.A., Coloma, L.A., O'Connell, L.A., 2016. Ant and mite diversity drives toxin variation in the little devil poison frog. *J. Chem. Ecol.* 42, 537–551. <http://dx.doi.org/10.1007/s10886-016-0715-x>.
- Medina, I., Wang, J.J., Salazar, C., Amézquita, A., 2013. Hybridization promotes color polymorphism in the aposematic harlequin poison frog, *Oophaga histrionica*. *Ecol. Evol.* 3, 4388–4400. <http://dx.doi.org/10.1002/ece3.794>.
- Merrill, R.M., Chia, A., Nadeau, N.J., 2014. Divergent warning patterns contribute to assortative mating between incipient *Heliconius* species. *Ecol. Evol.* 4, 911–917. <http://dx.doi.org/10.1002/ece3.996>.
- Myers, N., Mittermeier, R.A., Mittermeier, R.C.G., de Fonseca, G.A., Kent, J., 2000. Biodiversity hotspots for conservation priorities. *Nature* 403, 853–858. <http://dx.doi.org/10.1038/35002501>.
- Noble, G.K., 1921. Five new species of Salientia from South America. *Am. Museum Novit.* 29, 1–7.
- Oksanen, J., Blanchet, F.G., Friendly, M., Kindt, R., Legendre, P., McGlenn, D., Minchin, P.R., O'Hara, R.B., Simpson, G.L., Solymos, P., Stevens, M.H.H., Szoezs, E., Wagner, H., 2016. *vegan: community ecology package*. R package version 2.4-1. <<https://CRAN.R-project.org/package=vegan>>.
- Ortega-Andrade, H.M., Rojas-Soto, O.R., Valencia, J.H., Espinosa de los Monteros, A., Morrone, J.J., Ron, S.R., Cannatella, D.C., 2015. Insights from integrative systematics reveal cryptic diversity in *Pristimantis* frogs (Anura: Craugastoridae) from the upper Amazon Basin. *PLoS ONE* 10, 1–43. <http://dx.doi.org/10.1371/journal.pone.0143392>.
- Padial, J.M., De La Riva, I., 2009. Integrative taxonomy reveals cryptic Amazonian species of *Pristimantis* (Anura: Strabomantidae). *Zool. J. Linn. Soc.* 155, 97–122. <http://dx.doi.org/10.1111/j.1096-3642.2008.00424.x>.
- Pamilo, P., Nei, M., 1988. Relationships between gene trees and species trees. *Mol. Biol. Evol.* 5, 568–583.
- Perez-Peña, P.E., Chavéz, G., Twomey, E., Brown, J.L., 2010. Two new species of *Ranitomeya* (Anura: Dendrobatidae) from eastern Amazonian Peru. *Zootaxa* 2439, 1–23.
- Posso-Terranova, A., Andrés, J.A., 2016. Complex niche divergence underlies lineage diversification in *Oophaga* poison frogs. *J. Biogeogr.* 2002–2015. <http://dx.doi.org/10.1111/jbi.12799>.
- Poulin, B., Lefebvre, G., Ibañez, R., Jaramillo, C., Hernández, C., Rand, A.S., 2001. Avian predation upon lizards and frogs in a neotropical forest understory. *J. Trop. Ecol.* 17, 21–40. <http://dx.doi.org/10.1017/S026646740100102X>.
- Przecek, K., Mueller, C., Vamosi, S.M., 2008. The evolution of aposematism is accompanied by increased diversification. *Integr. Zool.* 3, 149–156. <http://dx.doi.org/10.1111/j.1749-4877.2008.00091.x>.
- R Core Team, 2016. R: A Language and Environment for Statistical Computing. R Foundation for Statistical Computing, Vienna, Austria. <<https://www.R-project.org/>>.

- Rannala, B., Yang, Z., 2003. Bayes estimation of species divergence times and ancestral population sizes using DNA sequences from multiple loci. *Genetics* 1656, 1645–1656.
- Reid, N.M., Carstens, B.C., 2012. Phylogenetic estimation error can decrease the accuracy of species delimitation: a Bayesian implementation of the general mixed Yule-coalescent model. *BMC Evol. Biol.* 12, 196. <http://dx.doi.org/10.1186/1471-2148-12-196>.
- Rodríguez, A., Poth, D., Schulz, S., Gehara, M., Vences, M., 2013. Genetic diversity, phylogeny and evolution of alkaloid sequestering in Cuban miniaturized frogs of the *Eleutherodactylus limbatus* group. *Mol. Phylogenet. Evol.* 68, 541–554. <http://dx.doi.org/10.1016/j.ympev.2013.04.031>.
- Ronquist, F., Huelsenbeck, J.P., 2003. MrBayes 3: Bayesian phylogenetic inference under mixed models. *Bioinformatics* 19, 1572–1574. <http://dx.doi.org/10.1093/bioinformatics/btg180>.
- Ronquist, F., Teslenko, M., Van Der Mark, P., Ayres, D.L., Darling, A., Höhna, S., Larget, B., Liu, L., Suchard, M.A., Huelsenbeck, J.P., 2012. MrBayes 3.2: Efficient Bayesian phylogenetic inference and model choice across a large model space. *Syst. Biol.* 61, 539–542. <http://dx.doi.org/10.1093/sysbio/sys029>.
- Ryan, M.J., Rand, A.S., 2001. Feature weighting in signal recognition and discrimination by túngara frogs. In: Ryan, M.J. (Ed.), *Anuran Communication*. Smithsonian, Washington, DC, pp. 86–101.
- Santos, J.C., 2012. Fast molecular evolution associated with high active metabolic rates in poison frogs. *Mol. Biol. Evol.* 29, 2001–2018. <http://dx.doi.org/10.1093/molbev/mss069>.
- Santos, J.C., Baquero, M., Barrio Amorós, C.L., Coloma, L.A., Erdtmann, L.K., Lima, A.P., Cannatella, D.C., 2014. Aposematism increases acoustic diversification and speciation in poison frogs. *Proc. R. Soc. B Biol. Sci.* 281, 20141761. <http://dx.doi.org/10.1098/rspb.2014.1761>.
- Santos, J.C., Cannatella, D.C., 2011. Phenotypic integration emerges from aposematism and scale in poison frogs. *Proc. Natl. Acad. Sci. USA* 108, 6175–6180. <http://dx.doi.org/10.1073/pnas.1010952108>.
- Santos, J.C., Coloma, L.A., Cannatella, D.C., 2003. Multiple, recurring origins of aposematism and diet specialization in poison frogs. *Proc. Natl. Acad. Sci. USA* 100, 12792–12797. <http://dx.doi.org/10.1073/pnas.2133521100>.
- Santos, J.C., Coloma, L.A., Summers, K., Caldwell, J.P., Ree, R., Cannatella, D.C., 2009. Amazonian amphibian diversity is primarily derived from late Miocene Andean lineages. *PLoS Biol.* 7, 0448–0461. <http://dx.doi.org/10.1371/journal.pbio.1000056>.
- Santos, J.C., Tarvin, R.D., O'Connell, L.A., 2016. A review of chemical defense in poison frogs (Dendrobatidae): ecology, pharmacokinetics, and autoresistance. Schulte, B.A., Goodwin, T.E., Ferkin, M.H. (Eds.), *Chemical Signals in Vertebrates 13*, Springer Science + Business Media, New York, pp. 305–337. <http://dx.doi.org/10.1007/978-0-387-73945-8>.
- Saporito, R.A., Donnelly, M.A., Jain, P., Garraffo, H.M., Spande, T.F., Daly, J.W., 2007. Spatial and temporal patterns of alkaloid variation in the poison frog *Oophaga pumilio* in Costa Rica and Panama over 30 years. *Toxicon* 50, 757–778. <http://dx.doi.org/10.1016/j.toxicon.2007.06.022>.
- Saporito, R.A., Donnelly, M.A., Spande, T.F., Garraffo, H.M., 2012. A review of chemical ecology in poison frogs. *Chemoecology* 22, 159–168. <http://dx.doi.org/10.1007/s00049-011-0088-0>.
- Schneider, C.A., Rasband, W.S., Eliceiri, K.W., 2012. NIH Image to ImageJ: 25 years of image analysis. *Nat. Methods* 9, 671–675. <http://dx.doi.org/10.1038/nmeth.2089>.
- Sillen-Tullberg, B., Bryant, E.H., 1983. The evolution of aposematic coloration in distasteful prey: an individual selection model. *Evolution* 37, 993–1000.
- Stamatakis, A., 2014. RAxML version 8: a tool for phylogenetic analysis and post-analysis of large phylogenies. *Bioinformatics* 30, 1312–1313. <http://dx.doi.org/10.1093/bioinformatics/btu033>.
- Stephens, M., Donnelly, P., 2003. A comparison of Bayesian methods for haplotype reconstruction from population genotype data. *Am. J. Hum. Genet.* 73, 1162–1169. <http://dx.doi.org/10.1086/379378>.
- Stephens, M., Smith, N.J., Donnelly, P., 2001. A new statistical method for haplotype reconstruction from population data. *Am. J. Hum. Genet.* 68, 978–989. <http://dx.doi.org/10.1086/319501>.
- Stuart, S.N., Chanson, J.S., Cox, N.A., Young, B.E., Rodrigues, A.S.L., Fischman, D.L., Waller, R.W., 2004. Status and trends of amphibian declines and extinctions worldwide. *Science* 306, 1783–1786. <http://dx.doi.org/10.1126/science.1103538>.
- Summers, K., Cronin, T.W., Kennedy, T., 2004. Cross-breeding of distinct color morphs of the strawberry poison frog (*Dendrobates pumilio*) from the Bocas del Toro Archipelago, Panama. *J. Herpetol.* 38, 1–8. <http://dx.doi.org/10.1670/51-03A>.
- Swofford, D.L., 2002. PAUP*: Phylogenetic Analysis Using Parsimony (*and Other Methods) v. 4.0a140. Sinauer Assoc. Sunderland, Massachusetts.
- Tarvin, R.D., Santos, J.C., O'Connell, L.A., Zakon, H.H., Cannatella, D.C., 2016. Convergent substitutions in a sodium channel suggest multiple origins of toxin resistance in poison frogs. *Mol. Biol. Evol.* 33, 1068–1081. <http://dx.doi.org/10.1093/molbev/msv350>.
- Tarvin, R.D., Santos, J.C., Ron, S.R., Cannatella, D.C., Visual signal evolution in *Epipedobates* poison frogs during early stages of aposematism. *Evolution*, In review.
- Toledo, L.F., Haddad, C.F.B., 2009. Colors and some morphological traits as defensive mechanisms in anurans. *Int. J. Zool.* 2009, 1–12. <http://dx.doi.org/10.1155/2009/910892>.
- Vences, M., Chiari, Y., Raharivololainaina, L., Meyer, A., 2004. High mitochondrial diversity within and among populations of Malagasy poison frogs. *Mol. Phylogenet. Evol.* 30, 295–307. [http://dx.doi.org/10.1016/S1055-7903\(03\)00217-3](http://dx.doi.org/10.1016/S1055-7903(03)00217-3).
- Vences, M., Kosuch, J., Boistel, R., Haddad, C.F.B., La Marca, E., Lötters, S., Veith, M., 2003. Convergent evolution of aposematic coloration in Neotropical poison frogs: a molecular phylogenetic perspective. *Org. Divers. Evol.* 3, 215–226. <http://dx.doi.org/10.1078/1439-6092-00076>.
- Vieites, D.R., Wollenberg, K.C., Andreone, F., Köhler, J., Glaw, F., Vences, M., 2009. Vast underestimation of Madagascar's biodiversity evidenced by an integrative amphibian inventory. *Proc. Natl. Acad. Sci. USA* 106, 8267–8272. <http://dx.doi.org/10.1073/pnas.0810821106>.
- Wang, I.J., 2011. Inversely related aposematic traits: reduced conspicuity evolves with increased toxicity in a polymorphic poison-dart frog. *Evolution* 65, 1637–1649. <http://dx.doi.org/10.1111/j.1558-5646.2011.01257.x>.
- Wang, I.J., Shaffer, H.B., 2008. Rapid color evolution in an aposematic species: a phylogenetic analysis of color variation in the strikingly polymorphic strawberry poison-dart frog. *Evolution* 62, 2742–2759. <http://dx.doi.org/10.1111/j.1558-5646.2008.00507.x>.
- Wells, K.D., 2007. *The Ecology and Behavior of Amphibians*, first ed. The University of Chicago Press, Chicago. <http://dx.doi.org/10.1017/CBO9781107415324.004>.
- Yang, Y., Richards-Zawacki, C.L., Devar, A., Dugas, M.B., 2016. Poison frog color morphs express assortative mate preferences in allopatry but not sympatry. *Evolution* 70, 2778–2788. <http://dx.doi.org/10.1111/evo.13079>.
- Yang, Z., 2015a. A tutorial of BPP for species tree estimation and species delimitation. *Curr. Zool.* 61, 854–865. <http://dx.doi.org/10.1093/czoolo/61.5.854>.
- Yang, Z., 2015b. BP&P Manual Version 3.1, <<http://abacus.gene.ucl.ac.uk/software/>>.
- Yang, Z., Rannala, B., 2010. Bayesian species delimitation using multilocus sequence data. *Proc. Natl. Acad. Sci. USA* 107, 9264–9269. <http://dx.doi.org/10.1073/pnas.0913022107>.
- Zhang, C., Zhang, D.X., Zhu, T., Yang, Z., 2011. Evaluation of a Bayesian coalescent method of species delimitation. *Syst. Biol.* 60, 747–761. <http://dx.doi.org/10.1093/sysbio/syr071>.